*29th EPS Conference on Plasma Phys. and Contr. Fusion Montreux, 17-21 June 2002 ECA Vol. **26B**, P-4.078 (2002)*

Transport Barriers in Braided Toroidal Magnetic Field

S. V. Kasilov[1], D. Reiter[2], A. M. Runov[3], W. Kernbichler[4], and M. F. Heyn[4]

[1]*Institute of Plasma Physics, National Science Center "Kharkov Institute of Physics and Technology", ul. Akademicheskaya 1, 61108 Kharkov, Ukraine*
[2]*Institut für Plasmaphysik, Forschungszentrum Jülich GmbH, EURATOM Association, Trilateral Euregio Cluster, D-52425 Jülich, Germany*
[3]*Institut für Plasmaphysik, Teilinstitut Greifswald, EURATOM Association, D-17491 Greifswald, Germany*
[4]*Institut für Theoretische Physik, Technische Universität Graz, Petersgasse 16, A–8010 Graz, Austria*

1. Introduction. In various tokamak experiments, strong internal electron transport barriers (ITBs) have been observed in regimes with reversed shear (see, e.g. [1,2]) if the q-minimum value approaches a low order rational number. Here, together with the fact that a low shear value dis-joins resonant perturbations of the limited radial width [3], the non-uniformity of the distribution of rational numbers with limited integer denominators [4] plays an important role. During the recent modelling of ion turbulence [5], using the fact that low order rational numbers, n_0/m_0 (integer m_0, n_0), stay at the distance of the order of $1/(m_0\bar{m})$ from all other rational numbers with denominators below $\bar{m}$, it has been shown that the gap between the resonant modes in the vicinity of the q reversal point is the biggest if the q-minimum value is near a low order rational.
In case of a monotonous q-profile, the electron ITBs have been observed in the experiments on RTP tokamak near low order rational surfaces [6]. The phenomenological analysis [7] using a model with a locally stepwise reduced electron heat conductivity around rational surfaces describes these observations quite well. The fact that it is the electron temperature which shows the barrier feature suggests that a possible reason for the formation of ITBs in RTP is the local reduction of the anomalous transport caused by magnetic field perturbations. In a recent analysis on the possibility of barrier formation in case of a monotonous q profile using a "tokamap" model for the perturbed magnetic field [8], barriers have been identified near broken KAM surfaces with "most noble" values of the rotational transform. In the present report, results are presented which are based on the studies of transport barriers in case of a monotonous q profile and static magnetic field perturbations with broad poloidal and toroidal spectra [9] where these barriers have been found near low order rational magnetic surfaces.

2. Magnetic field model. The simplified tokamak geometry is represented by a straight periodic cylinder where the azimuth θ is the poloidal angle and the coordinate along the z-axis is the toroidal angle $\varphi \equiv z/R_0$, with $2\pi R_0$ being the cylinder period. For the numerical modelling, the main magnetic field has been assumed to have constant shear, $\iota \equiv 1/q = r$, where $0 < r < 1$ is a dimensionless radius. The perturbation field $\mathbf{b} = \mathbf{B}/B_\varphi$ is derived from a static vector potential of the form

$$\mathbf{A} = \mathbf{e}_z A_z, \quad A_z \equiv A_\varphi = \frac{\epsilon r B_\varphi}{\bar{m}} \sum_{m=-M}^{M} \sum_{n=-N}^{N} a_{m,n} \sin(m\theta - n\varphi + \alpha_{mn}), \tag{1}$$

where $B_\varphi = const$, $\alpha_{m,n}$ are random phases, $M \gg 1$, $N \gg 1$ and $\bar{m} \gg 1$ is the poloidal spectral width. The Fourier amplitudes of b_r are obtained as $b_{m,n} = \epsilon a_{m,n} m/\bar{m}$. Two kinds of

spectra are considered in the following, a "simplified" spectrum with $a_{m,n} = 1$ and $M = N = \bar{m} = \bar{n}$, and a "realistic" spectrum with $a_{m,n} = \exp\left(-m^2/\bar{m}^2 - n^2/\bar{n}^2\right)$, $M > \bar{n}$ and $N > \bar{n}$. For small perturbation amplitudes, ϵ, near a given resonant magnetic surface with $\iota_0 = n_0/m_0$, an island structure is formed. The radial width of this structure is determined by all harmonics with the same helicity, $m = km_0$, $n = kn_0$, where $k = \pm 1, \pm 2, \ldots$. The equation for the magnetic surfaces takes the following form,

$$\frac{1}{R_0}\int_0^r \mathrm{d}r' r' \left(\frac{n_0}{m_0} - \iota(r')\right) + \sum_k \frac{r}{km_0} b_{km_0,kn_0} \sin\left(k(m_0\theta - n_0\varphi) + \alpha_{km_0,kn_0}\right) = const. \quad (2)$$

For an estimate of the sum in the second term in (2), it is assumed that the constant phase values $\alpha_{m,n}$ are random. Thus, for the "simplified" model one obtains the island width as

$$\delta r_{m_0,n_0} \approx 2\left(\frac{R_0|b_{m_0,n_0}|}{|m_0\iota'|}\right)^{1/2}\left(\frac{2\bar{m}}{m_0}\log\left(\frac{\bar{m}}{m_0}\right)\right)^{1/4} \sim \frac{\epsilon^{1/2}R_0^{1/2}}{|\iota'|^{1/2}\, m_0^{1/4}\bar{m}^{1/4}}\left(\log\left(\frac{\bar{m}}{m_0}\right)\right)^{1/4}, \quad (3)$$

where $\iota' \equiv \mathrm{d}\iota/\mathrm{d}r$. The estimate for the "realistic" model differs by a factor of order one. One can check that the second estimate in (3) stays valid in the more general case, where the $b_{m,n}$ scale with the perpendicular wavenumber as $\left(k_\perp/\bar{k}_\perp\right)^\gamma$ (so that $b_{m,n} \approx \epsilon(m/\bar{m})^\gamma$) and rapidly saturate for $k_\perp > \bar{k}_\perp$, as long as $\gamma > 1/2$. If $\gamma < 1/2$ the width of the island structure is completely defined by the main harmonic, $\delta r_{m_0,n_0} \approx 2\left|R_0 b_{m_0,n_0}\right|^{1/2}\left|m_0\iota'\right|^{-1/2} \sim \epsilon^{1/2}R_0^{1/2}\left|\iota'\right|^{-1/2} m_0^{(\gamma-1)/2}\bar{m}^{-\gamma/2}$. The radial distance between the position of the resonant mode $\iota = n_0/m_0$ and the nearest resonant mode which still has a significant amplitude value (the modes with m above the spectrum cut-off are negligible) is $\Delta r \approx (|\iota'|m_0\bar{m})^{-1}$ (see [5,9]). Since in all cases the lower order island structures are the widest, it is sufficient to take into account for the computation of Chirikov overlap criterion only the width of the lower order island structure. Relating this width to the distance between the resonances, and taking the square of this quantity one obtains

$$\sigma_b = 4\cdot 2^{1/2}|\iota'|R_0 b_{m_0,n_0}\bar{m}^{5/2}m_0^{1/2}\log^{1/2}(\bar{m}/m_0) \sim \epsilon|\iota'|R_0\left(m_0\bar{m}\right)^{3/2}\log^{1/2}(\bar{m}/m_0). \quad (4)$$

The second estimate is valid also for more general spectra with $\gamma > 1/2$. For $\gamma < 1/2$ one obtains in a similar way

$$\sigma_b \sim \epsilon|\iota'|R_0 m_0^{\gamma+1}\bar{m}^{2-\gamma}. \quad (5)$$

If $\sigma_b \gg 1$ the island structures overlap and form an ergodic magnetic field region. In the opposite case, one can expect more regular magnetic field behaviour in the Δr vicinity of the resonance $\iota = m_0/n_0$. It can be seen from Eqs. (4) and (5) that whenever $\gamma > -1$ the overlapping of the high order resonances occurs first. As a result, in the vicinities of low order resonance surfaces, barrier regions should persist while most of the tokamak volume is occupied by the ergodic regions. This is confirmed in Figs. 1 and 2 where the results of Poincaré mappings are compared with predictions of the overlapping analysis for the simplified magnetic field model.

3. Electron heat transport. The MHD transport properties of the chosen magnetic configurations have been studied numerically. The 3D Monte-Carlo fluid code E3D [10] has been used to solve the problem of heat conductivity described by

$$\frac{\partial T_e}{\partial t} - \nabla\cdot\left(D_\perp\nabla T_e + \left(D_\parallel - D_\perp\right)\mathbf{hh}\cdot\nabla T_e\right) = 0, \quad (6)$$

where $\mathbf{h} = \mathbf{B}/B$. The stationary problem of heat propagation from a constant source at the inner boundary located at $r = 0.4$ to an outer surface (the "wall") located at $r = 0.6$ is studied. The boundary condition at the wall is set to $T_e = 0$. A constant input heat flux $Q = 40$ W is prescribed at the inner boundary. The background plasma parameters are $T_e = 25$ eV, $n_e = 10^{13}$ cm^{-3}, and $D_\perp = 23$ cm^2 s^{-1} that is $1.45 \cdot 10^9$ times smaller than the classical parallel heat diffusion coefficient $D_\parallel$. In Figs. 3 and 4 the radial profiles of temperature averaged over both the poloidal and the toroidal angles are shown. Figs. 3, 4 and 5 correspond to the "simplified" model of the magnetic field with $\bar{m} = 20$ while Fig. 6 corresponds to the "realistic" model with $\bar{m} = \bar{n} = 10$. The calculated temperature gradient is significantly higher in "barrier" regions than in the "ergodic" shaded regions. "Barrier" regions are separated by the "plateau" region with a very small temperature gradient. This region is formed at the place of the island chain corresponding to the "main" helicity resonance $m_0 = 2$, $n_0 = 1$. In Figs. 5 and 6 the effective "diffusion" coefficient computed from the averaged temperature profile and normalized to $D_\perp$,

$$\frac{D_{\text{eff}}}{D_\perp} = -\frac{Q}{4\pi^2 R_0 r D_\perp} \left(\frac{\mathrm{d}T_e}{\mathrm{d}r} \right)^{-1}, \tag{7}$$

is compared to the normalized Rechester-Rosenbluth diffusion coefficient. One can see that effective diffusion coefficients scale according to the Rechester-Rosenbluth theory and drop in the "barrier" region.

Thus, the MHD modeling confirms the presence of transport barriers in case of a monotonous q profile. Note that the scaling of the criterion (4) with parameters is independent of the shape of the perpendicular (poloidal) spectrum of $b_{m,n} \leq 1$ as long as the $b_{m,n}$ increase faster with respect to $k_\perp$ than $k_\perp^{1/2}$ up to the spectrum cut-off. Actually, the same is true also for the quasilinear field line diffusion coefficient and the Kolmogorov length (see [11]), and, therefore, also for the Rechester-Rosenbluth diffusion coefficient D_{RR}. Therefore, in the presence of an electron transport barrier in case of a monotonous q-profile and assuming that the observed electron diffusion is in the Rechester-Rosenbluth regime, one can roughly estimate the upper limit of $\bar{k}_\perp$, the spectral width of the perturbations using (4) and putting D_{RR} to the observed anomalous value [9]. For the parameters of RTP [1], $\bar{k}_\perp < 9$ cm^{-1} is obtained. This correlates with the skin depth.

[1] F. Alladio, et al, Plasma Phys. Contr. Fusion **41** (1999) A323-A332.

[2] K. A. Razumova, et al, Plasma Phys. Contr. Fusion **42** (2000) 973-986.

[3] F. Romanelli and F. Zonca, Phys. Fluids B **5** (1993) 4081-4089.

[4] A. D. Beklemishev and W. Horton, Phys. Fluids B **4** (1992) 200-206.

[5] X. Garbet, Phys. Plasmas **8** (2001) 2793-2803.

[6] J. Gorini, et al, Plasma Phys. and Contr. Fusion, **42**(suppl.5A) (2000) A161-168.

[7] G. M. D. Hogeweij, et al, Nuclear Fusion **38** (1998) 1881-1891.

[8] J. H. Misguich, Phys. Plasmas **8** (2001) 2132-2138.

[9] S. V. Kasilov, et al, Plasma Phys. Contr. Fusion **44** (2002) 985-1004.

[10] A. M. Runov, et al, Phys. Plasmas **8** (2001) 916-930.

[11] J. A. Krommes, C. Oberman, and R. G. Kleva, J. Plasma Phys. **30** (1983) 11-56.

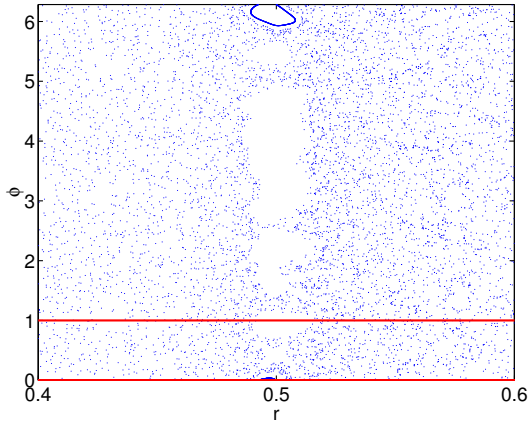

Figure 1. Poincaré plot of the magnetic field for $\bar{m} = 20$ and $\epsilon = 2.6666 \cdot 10^{-4}$.

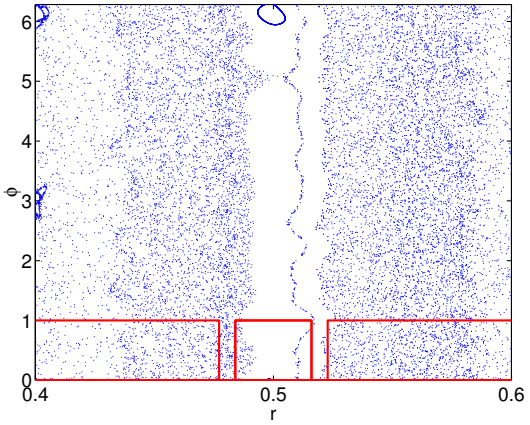

Figure 2. Same as Fig. 1 for $\epsilon = 1.3333 \cdot 10^{-4}$. The gap shown by the red line corresponds to the barrier zone.

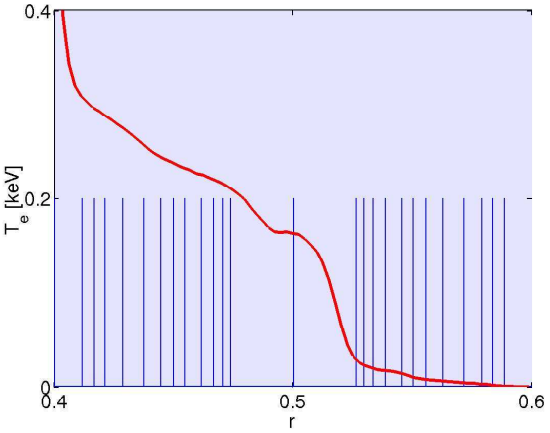

Figure 3. Temperature profile for "simplified" model with $\epsilon = 2.6666 \cdot 10^{-4}$ ($\sigma_b = 0.58$).

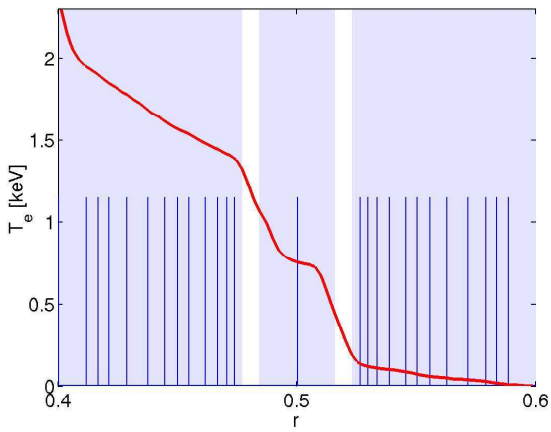

Figure 4. Same as Fig.3 for $\epsilon = 1.3333 \cdot 10^{-4}$ ($\sigma_b = 0.29$).

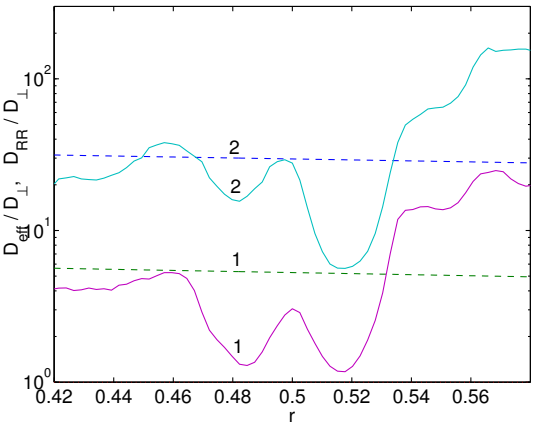

Figure 5. Normalized effective diffusion $D_{\rm eff}/D_\perp$ (solid) and Rechester-Rosenbluth (dashed) coefficients for the "simplified" magnetic field spectrum. Curves 1 - $\epsilon = 1.3333 \cdot 10^{-4}$, Curves 2 - $\epsilon = 2.6666 \cdot 10^{-4}$.

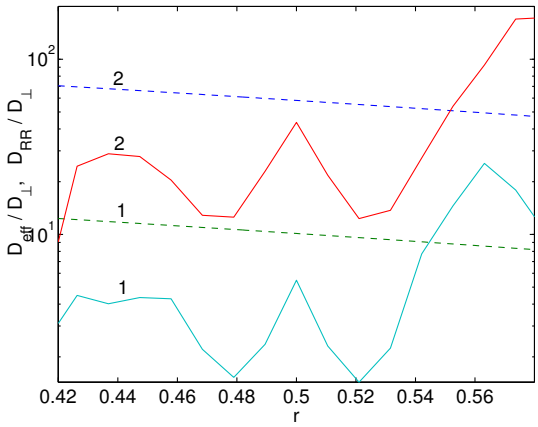

Figure 6. Normalized effective diffusion $D_{\rm eff}/D_\perp$ (solid) and Rechester-Rosenbluth (dashed) coefficients for the "realistic" magnetic field spectrum. Curves 1 - $\epsilon = 10^{-3}$, Curves 2 - $\epsilon = 5 \cdot 10^{-4}$.